

Supporting Information

Ultrasmall hybrid protein-copper sulfide nanoparticles for targeted photoacoustic imaging of orthotopic hepatocellular carcinoma with high signal-to-noise ratio

Huixiang Yan,^{†ab} Jingqin Chen,^{†bc} Ying Li,^d Yuanyuan Bai,^b Yunzhu Wu,^a Zonghai Sheng,^e Liang Song,^b Chengbo Liu,^{*b} and Hai Zhang^{*a}

^a *Department of Ultrasonography, The Second Clinical College of Jinan University, Shenzhen People's Hospital, 518020 Shenzhen, China*

^b *Research Laboratory for Biomedical Optics and Molecular Imaging, Shenzhen Key Laboratory for Molecular Imaging, Institute of Biomedical and Health Engineering, Shenzhen Institutes of Advanced Technology, Chinese Academy of Sciences, Shenzhen 518055, China.*

^c *Shenzhen College of Advanced Technology, University of Chinese Academy of Sciences, Shenzhen 518055, China.*

^d *Division of Radiology, Department of Medicine, the University of Hong Kong Shenzhen Hospital*

^e *Paul C. Lauterbur Research Center for Biomedical Imaging, Institute of Biomedical and Health Engineering, Shenzhen Institutes of Advanced Technology, Chinese Academy of Sciences, Shenzhen 518055, China.*

* Corresponding authors:

Chengbo Liu E-mail: cb.liu@siat.ac.cn. Tel: +86 (755) 8639-2240

Hai Zhang E-mail: szzhans.scc.jnu@foxmail.com. Tel: +86 (755) 2553-3497

† These authors contributed equally to this work.

Figure S1

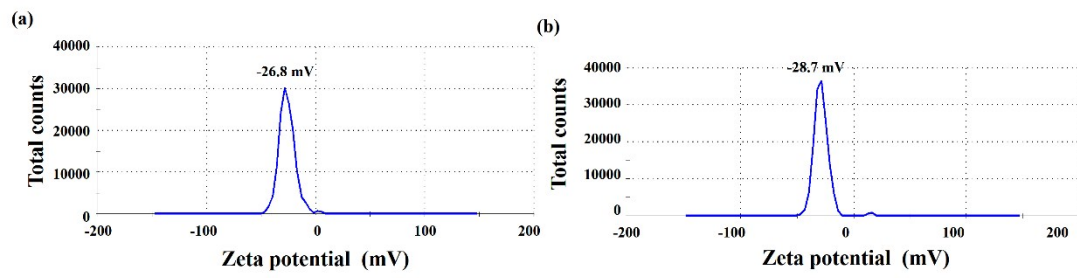


Figure S1. The zeta potential distribution of (a) CuS@BSA-RGD NPs and (b) CuS@BSA NPs.

Figure S2

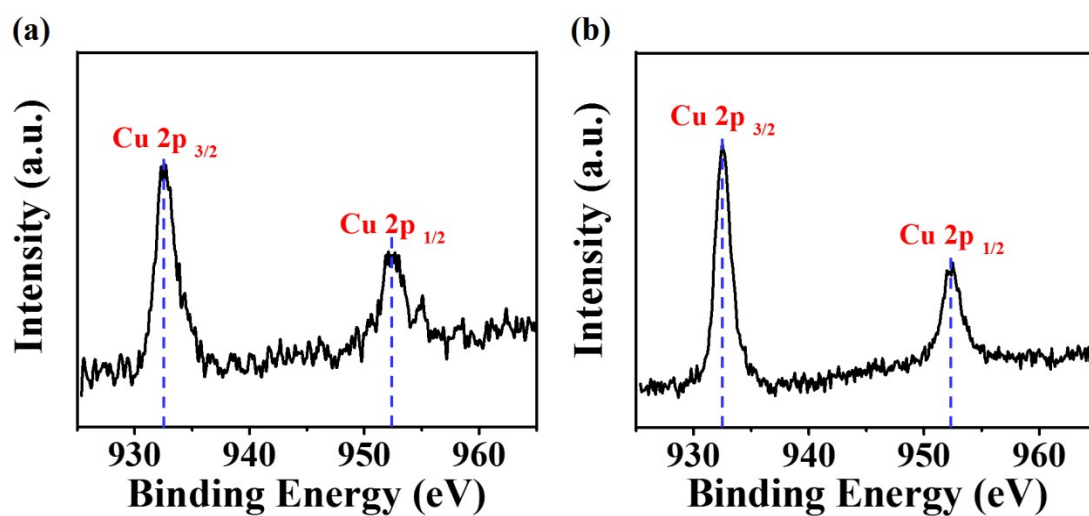


Figure S2. Cu 2p region X-ray photoelectron spectroscopy (XPS) spectra of (a) CuS@BSA-RGD NPs and (b) CuS@BSA NPs.

Figure S3

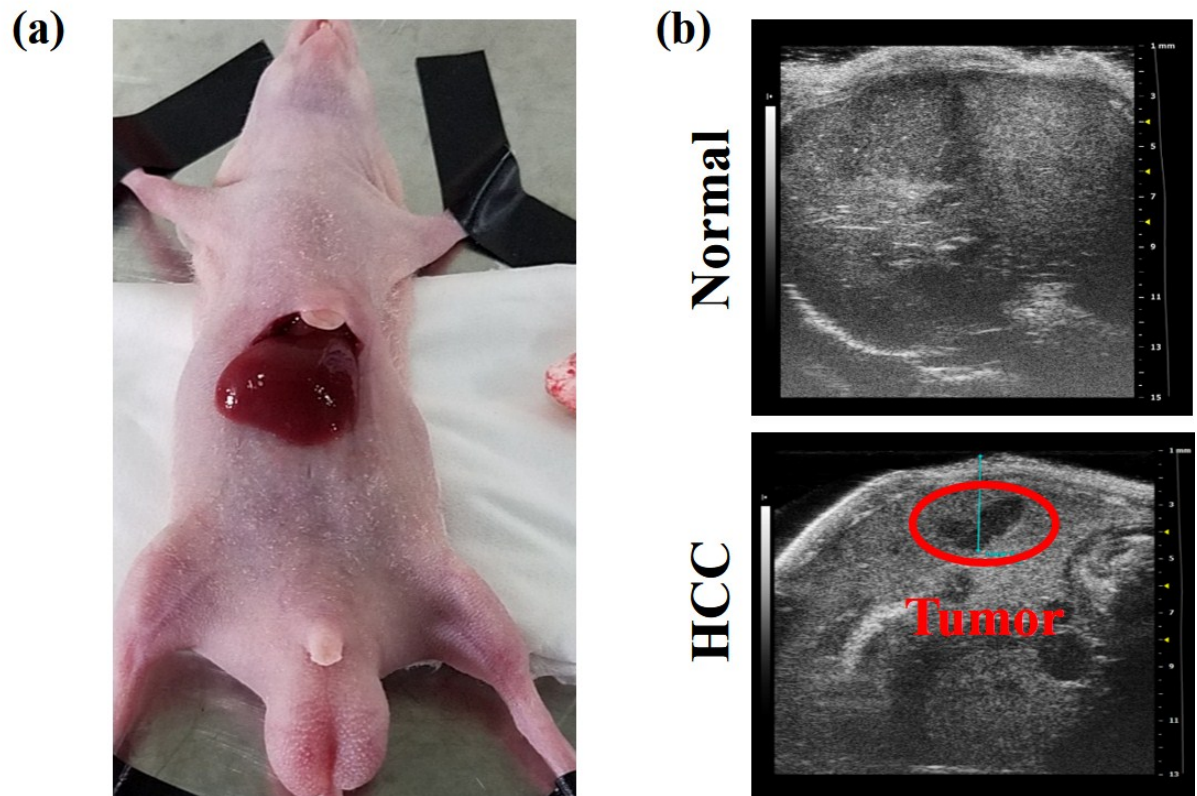


Figure S3. (a) The photograph of the normal mouse liver. (b) The ultrasound images of liver region in normal and HCC bearing mice. The red circle delineates the HCC region.

Figure S4

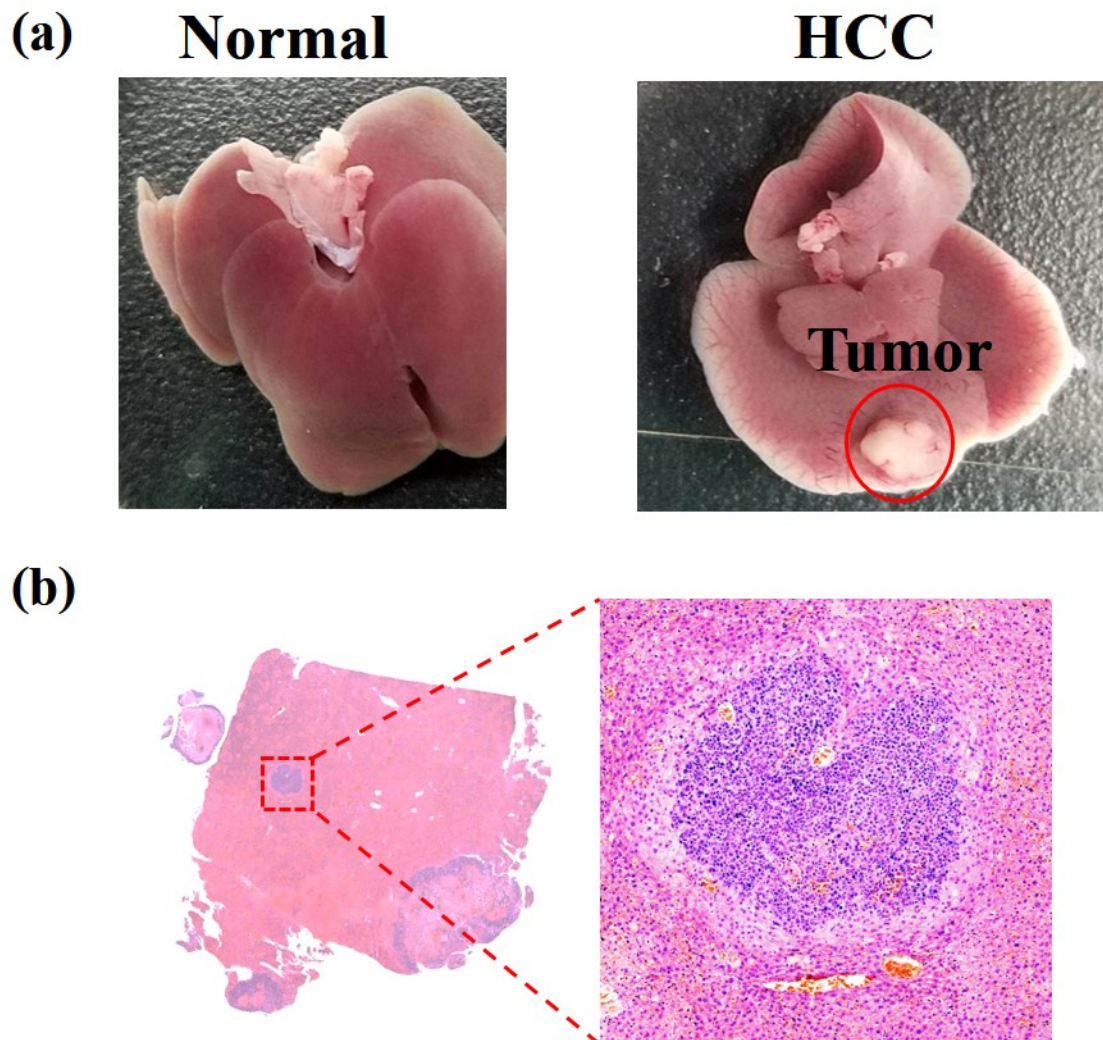


Figure S4. (a) The photograph of the normal and HCC bearing liver tissues. (b) The HE stained images of HCC bearing liver tissues. The red dotted square delineates the HCC region.

Figure S5

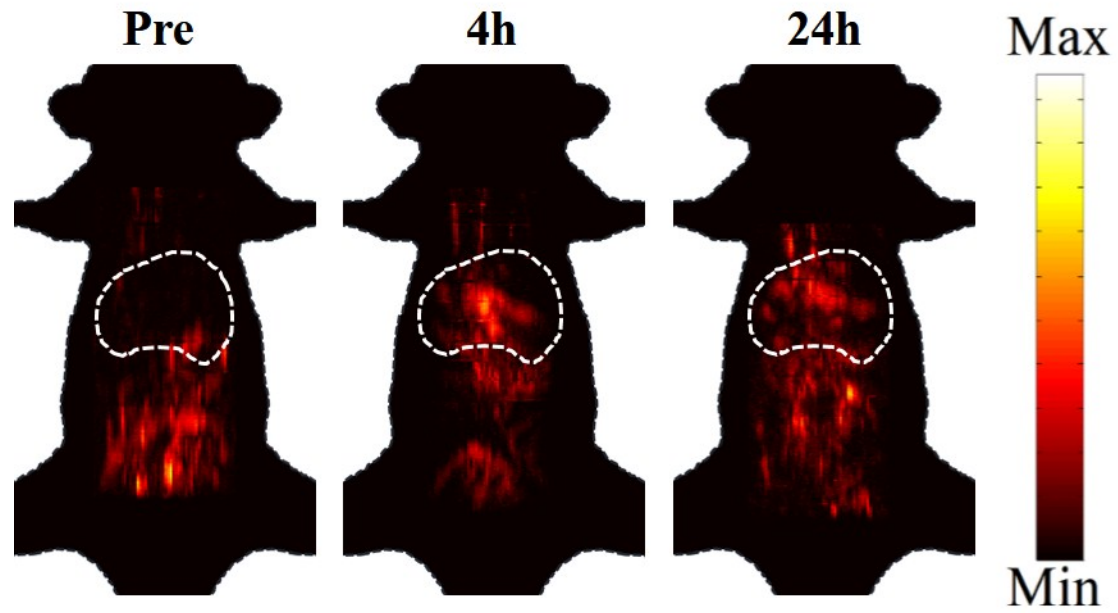


Figure S5. *In vivo* PA imaging of CuS@BSA NPs in orthotopic liver cancer model.

Figure S6

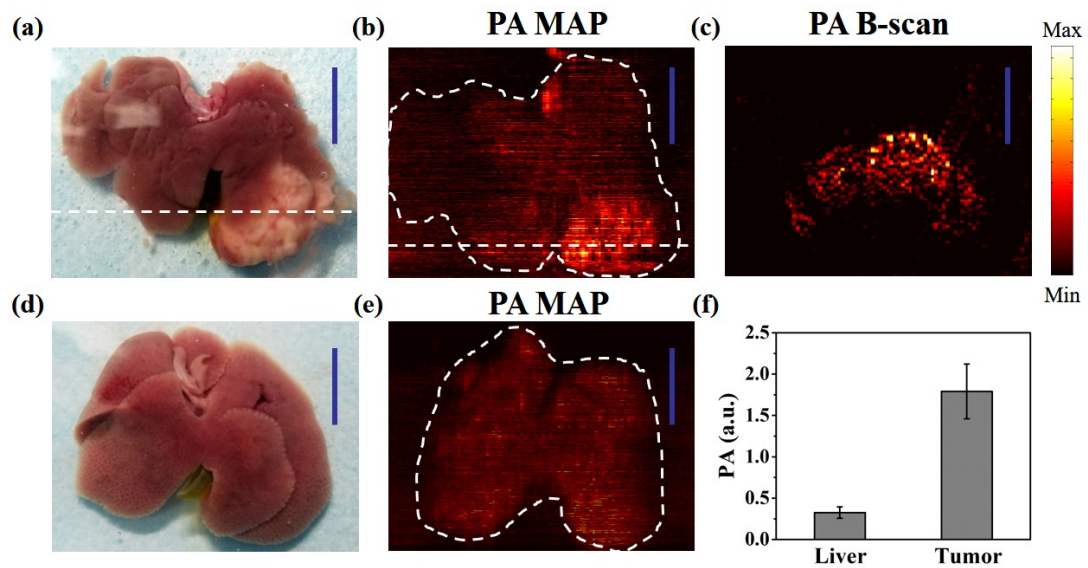


Figure S6. (a and b) Photograph and corresponding PA MAP image of liver in HCC bearing mouse. (c) The B-scan of white dash line region in (b). (d and e) Photograph and corresponding PA MAP image of normal liver. (f) The comparison of PA signals between health liver region and HCC region. (scale bar: 10 mm).

Figure S7

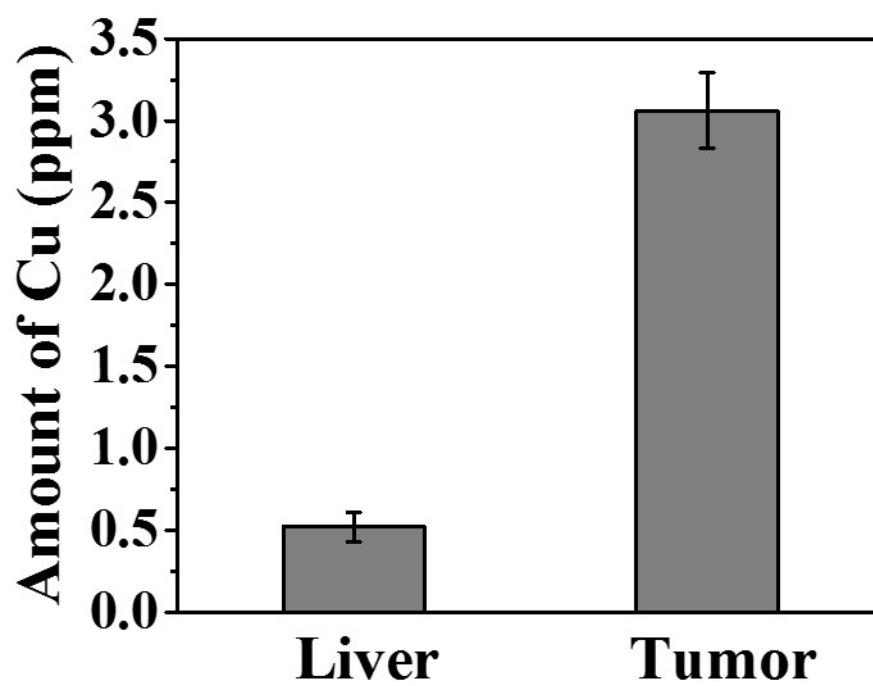


Figure S7. The amount of Cu in liver and tumor at 24 h post CuS@BSA-RGD NPs injection.

Figure S8

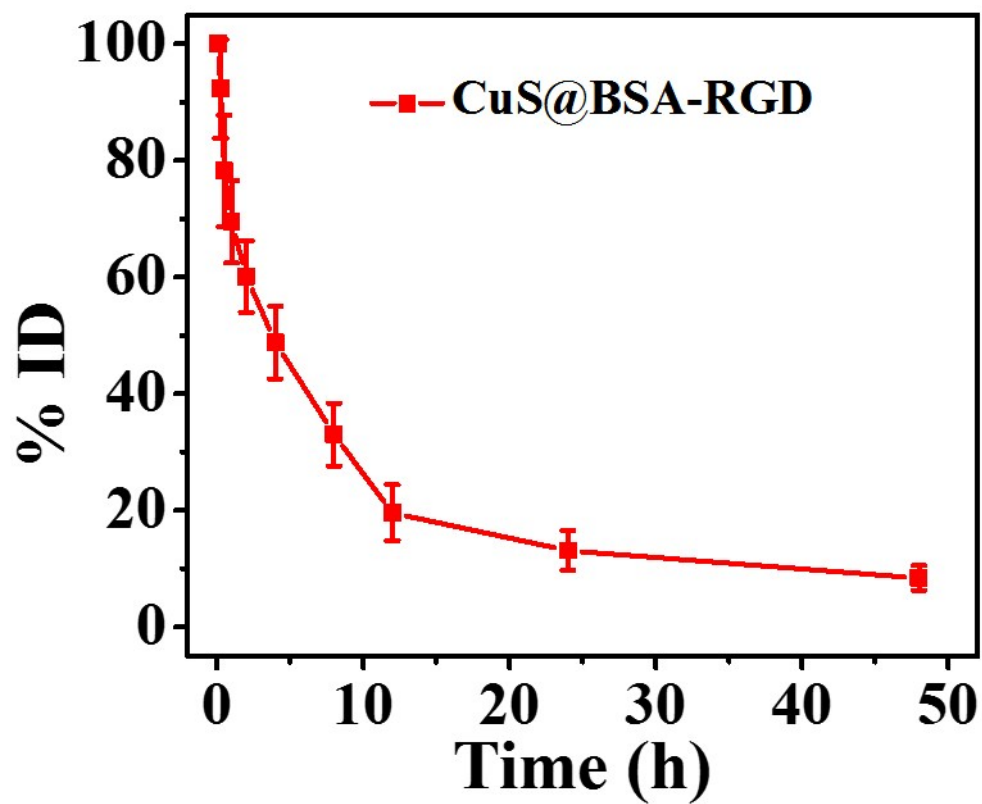


Figure S8. Blood circulation profile of CuS@BSA-RGD NPs.